Developmental Cell
Article

CASZ1 Promotes Vascular Assembly and Morphogenesis through the Direct Regulation of an EGFL7/RhoA-Mediated Pathway

Marta S. Charpentier,[1,3,6] Kathleen S. Christine,[1,2,6] Nirav M. Amin,[1,3] Kerry M. Dorr,[1,3] Erich J. Kushner,[2,5] Victoria L. Bautch,[1,2,3,5] Joan M. Taylor,[1,4] and Frank L. Conlon[1,2,3,5,*]
[1]McAllister Heart Institute
[2]Department of Biology
[3]Department of Genetics
[4]Department of Pathology and Laboratory Medicine
[5]Lineberger Comprehensive Cancer Center
University of North Carolina at Chapel Hill, Chapel Hill, NC 27599-3280, USA
[6]These authors contributed equally to this work
*Correspondence: frank_conlon@med.unc.edu
http://dx.doi.org/10.1016/j.devcel.2013.03.003

SUMMARY

The formation of the vascular system is essential for embryonic development and homeostasis. However, transcriptional control of this process is not fully understood. Here we report an evolutionarily conserved role for the transcription factor CASZ1 (CASTOR) in blood vessel assembly and morphogenesis. In the absence of CASZ1, *Xenopus* embryos fail to develop a branched and lumenized vascular system, and CASZ1-depleted human endothelial cells display dramatic alterations in adhesion, morphology, and sprouting. Mechanistically, we show that CASZ1 directly regulates *Epidermal Growth Factor-Like Domain 7* (*Egfl7*). We further demonstrate that defects of CASZ1- or EGFL7-depleted cells are in part due to diminished RhoA expression and impaired focal adhesion localization. Moreover, these abnormal endothelial cell behaviors in CASZ1-depleted cells can be rescued by restoration of *Egfl7*. Collectively, these studies show that CASZ1 is required to directly regulate an EGFL7/RhoA-mediated pathway to promote vertebrate vascular development.

INTRODUCTION

Endothelial cells (ECs) are building blocks for the formation of a functional vascular system during embryonic development. Early stages of blood vessel development occur via vasculogenesis, whereby mesodermal cells differentiate into EC progenitors that subsequently proliferate, migrate, and assemble into vascular cords. The cords then undergo tubulogenesis, or lumen formation, and continue to mature by angiogenesis, whereby vessels sprout, branch, and remodel. The vessels then become surrounded and stabilized by pericytes and smooth muscle cells that provide structural support (De Val, 2011; Patan, 2000). The critical nature of these events is emphasized by observations that disruption of these processes is associated with human disease states, including cancer, stroke, and atherosclerosis, highlighting the need for a better understanding of the transcriptional networks that regulate these key developmental steps (Carmeliet, 2003; Carmeliet and Jain, 2011; Potente et al., 2011).

Although numerous transcription factors have been discovered to regulate endothelial gene expression, relatively few factors are necessary for development. Deletions or mutations of a number of single genes, especially members of the Ets and forkhead families, result in moderate to no vascular phenotypes, likely due to functional redundancy (Barton et al., 1998; De Val, 2011; De Val and Black, 2009; Lelièvre et al., 2001). Previous studies have implicated the zinc finger transcription factor CASZ1 (CASTOR) in cardiovascular development, with depletion of CASZ1 in *Xenopus* embryos resulting in the failure of a subset of progenitor cells to differentiate into cardiomyocytes (Christine and Conlon, 2008). Recent genome-wide association studies have shown a genetic link between human *Casz1* and high blood pressure and hypertension, suggesting a possible role for CASZ1 in EC biology (Levy et al., 2009; Takeuchi et al., 2010). However, no studies have addressed the expression, function, or transcriptional targets of CASZ1 in vascular tissue.

Despite an essential role of the vasculature in development and disease, our knowledge about the molecular mechanisms that control these events remains incomplete (De Val and Black, 2009). One protein that was recently shown to play a role in EC morphogenesis is *Epidermal Growth Factor-Like Domain 7* (*Egfl7*), an extracellular matrix (ECM) protein that is expressed exclusively in EC progenitors and vessels during embryonic and neonatal development. EGFL7 is also expressed in highly vascularized adult organs and is upregulated upon injury (Campagnolo et al., 2005; Fitch et al., 2004; Parker et al., 2004). Depletion studies in zebrafish have defined a role for EGFL7 in tubulogenesis, likely through modulation of cell-matrix interactions (Nikolic et al., 2010; Parker et al., 2004). In addition, overexpression of *Egfl7* in mouse results in abnormal patterning of embryonic and postnatal vasculature (Nichol et al., 2010). However, efforts to identify the specific function of EGFL7 have been complicated by the recent discovery of microRNA

miR-126, the only EC-specific microRNA, within intron 7 of the *Egfl7* locus. Although *Egfl7* and miR-126 are coexpressed, miR-126 plays a role distinct from that of its host gene in maintaining vessel integrity and modulating angiogenesis through repression of the targets *Spred1* and *PIK3R2* (Fish et al., 2008; Kuhnert et al., 2008; Wang et al., 2008).

In this study, we demonstrate that CASZ1 is required for angiogenic sprouting and lumen morphogenesis. CASZ1 regulates EC contractility, adhesion, and sprouting, thereby promoting the assembly and tubulogenesis of blood vessels. Furthermore, we demonstrate that CASZ1 activates *Egfl7* in mammals and *Xenopus* by binding directly to an intronic element. However, CASZ1 regulates miR-126 in mammals but not in *Xenopus*. Moreover, defects associated with CASZ1 depletion can be phenocopied by EGFL7 depletion and, importantly, rescued by restoration of *Egfl7* levels. We further show CASZ1 transcriptional control of EGFL7 modulates EC behavior through RhoA. Collectively, our studies point to a network whereby CASZ1 regulates an EGFL7/RhoA-mediated pathway to promote vessel assembly and morphogenesis.

RESULTS

EC Expression of CASZ1 Is Evolutionarily Conserved

Analysis of *Casz1* expression in *Xenopus* embryos showed transcripts in the vitelline vein network at a stage when the network is primarily made up of vascular ECs and devoid of smooth muscle cells (Figure 1A; Christine and Conlon, 2008; Cox et al., 2006; Warkman et al., 2005), suggesting that *Casz1* is expressed in vascular ECs. Furthermore, RT-PCR on vascular explants from late-tailbud-stage embryos (stage 32) demonstrated that *Casz1* is coexpressed in the vitelline vein region with the vascular markers *Msr* and *Erg* (Figure S1A available online). Consistently, we found that CASZ1 colocalizes with the EC-specific marker PECAM in blood vessels of mouse embryos (Figure 1B). We went on to clone human *Casz1* and showed that *Casz1* is expressed in primary human umbilical vein ECs (HUVECs; Figures 1C and 1D). Together with the previously reported sequence homology and synteny of CASZ1 across vertebrates (Christine and Conlon, 2008), these results demonstrate that CASZ1 is an evolutionarily conserved transcription factor expressed in ECs.

CASZ1 Is Required for Vascular Patterning and Lumen Morphogenesis

To ascertain the function of CASZ1 in vascular development, we depleted CASZ1 in *Xenopus* embryos using a morpholino (MO)-based approach (Christine and Conlon, 2008). Whole-mount in situ hybridization using a panel of EC markers such as *Msr* and *Erg* (Baltzinger et al., 1999; Devic et al., 1996) demonstrated that at stages when ECs began to migrate dorsally from ventral blood islands within the trunk region, there were no noticeable differences between control and CASZ1-depleted embryos (stage 29; Figures S1B, S1C, S1J, and S1K). However, when ECs began to assemble into cords (stage 32), defects became apparent (e.g., CASZ1-depleted embryos displayed a dramatically reduced vascular plexus; Figures 2A–2D, S1D, and S1E). Extension of intersomitic vessels from posterior cardinal veins, which is known to occur in *Xenopus* via sprouting angiogenesis

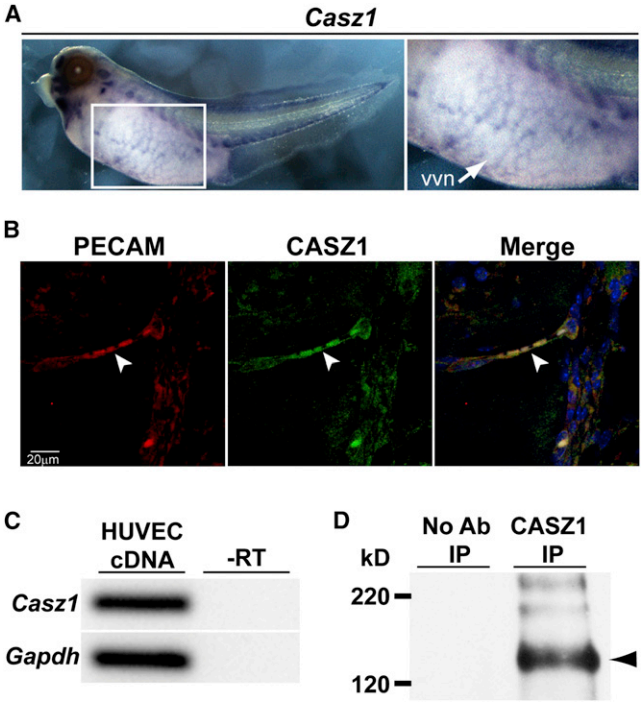

Figure 1. CASZ1 Expression in Vascular ECs Is Evolutionarily Conserved

(A) In situ analysis of *Casz1 Xenopus* embryos (stage 41; lateral view with anterior to the left). *Casz1* is expressed in vascular structures, including the vitelline vein network (vvn; enlarged panel on the right).

(B) CASZ1 (green) colocalizes with PECAM (red) in neural blood vessels of E14.5 mouse embryos.

(C) RT-PCR analysis of human *Casz1* in HUVEC cDNA. *Gapdh* was used as loading control.

(D) IP of CASZ1 from HUVECs. Control lane (left) represents IP with no antibody (Ab). Arrowhead represents 125 kD human CASZ1. See also Figure S1.

in an anterior-to-posterior direction (Cleaver et al., 1997; Levine et al., 2003), was also absent or significantly delayed in CASZ1-depleted embryos (Figures 2A, 2C, 2E, and 2G). By the mid- to late-tadpole stages (stages 36 and 39, respectively), the vascular networks of CASZ1-depleted embryos were comprised of cords that ran predominantly in a dorsal-to-ventral pattern and underwent little to no branching or remodeling (Figures 2E–2H, S1F–S1I, S1L, and S1M). Overall, at stage 36, the total length of the vitelline vein vasculature and the number of branch points and intersomitic vessels were all significantly decreased in CASZ1-depleted embryos (Figure 2I). While our studies focused on vein-derived sprouts, CASZ1 is unlikely to be required for arterial/venous specification based on observations that the aortic arches (arterial) and posterior cardinal veins are properly specified and positioned in CASZ-depleted embryos, and expression of arterial markers is absent in veins (data not shown). Collectively, these data imply a role for CASZ1 in sprouting and remodeling of the vasculature.

Noting that the posterior cardinal veins of CASZ1-depleted embryos appeared thickened (stage 36), we sought to determine the time course of lumen formation in *Xenopus*. At stage 29, control and CASZ1-depleted ECs, as marked by *Msr*, were localized to positions of the future veins but had not yet undergone lumen

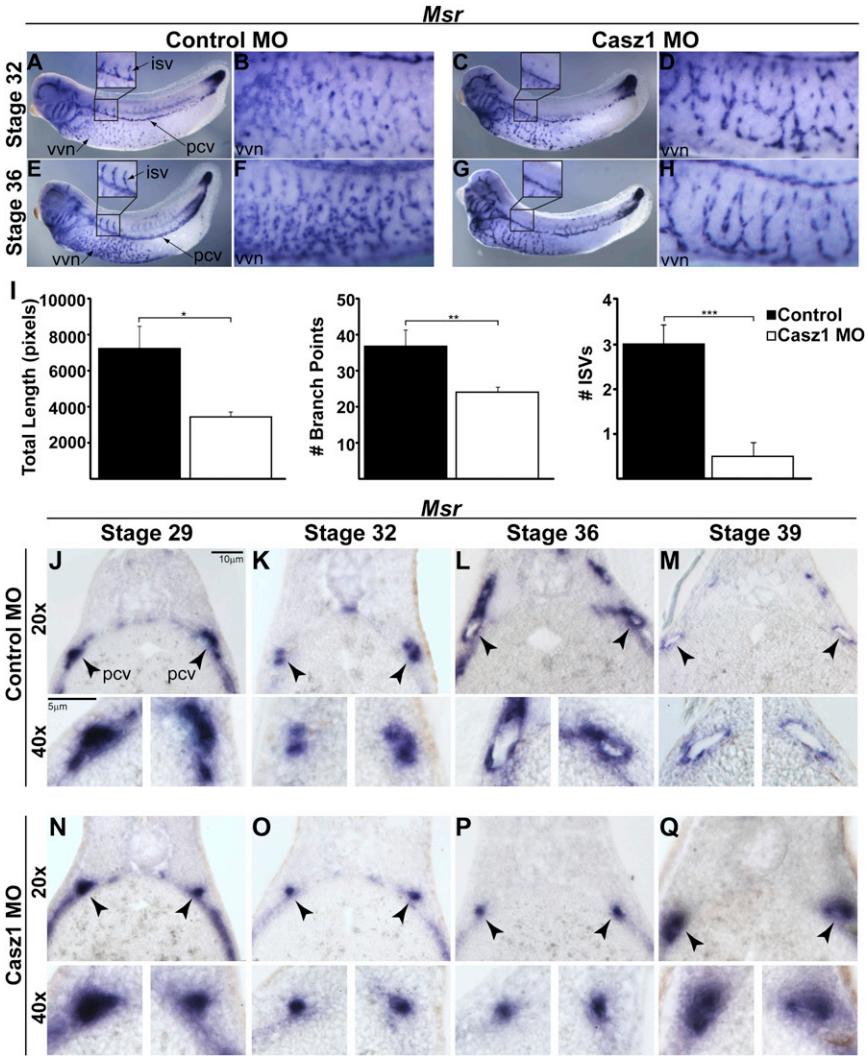

Figure 2. CASZ1 Is Required for Vascular Development and Lumen Formation

(A–H) In situ analysis with EC marker *Msr* of control and CASZ1-depleted embryos (stages 32–36; lateral view with anterior to the left). Vessel patterning and branching within the vvn are severely compromised at stage 32 in CASZ1-depleted embryos (A and C: high magnification of the vvn in B and D) and stage 36 (E and G: high magnification of the vvn in F and H). Note the poor sprouting of intersomitic vessels (isv) in CASZ1-depleted embryos at both stages (enlarged box in A, C, E, and G). n = 10 embryos/condition/stage, three independent experiments. pcv, posterior cardinal vein.

(I) Quantification of vascular defects in control and CASZ1-depleted embryos (stage 36) representing the combined total length of vessels, number of branch points within the vvn, and number of isv/embryo, respectively. Data represent mean ± SEM (n = 7 control and 10 Casz1 MO embryos). *p < 0.05, **p < 0.01, ***p < 0.001.

(J–Q) Histological analysis illustrates the time course of lumen formation in *Xenopus* from stage 29 to stage 39 (J–M). Note that posterior cardinal vein (pcv) lumens begin to open between stages 32 and 36 in control embryos (K and L) but fail to form in CASZ1-depleted embryos (N–Q). Dorsal is top, ventral is bottom. Arrowheads correspond to positions of pcv that are enlarged in lower panels (n = 2–5 embryos/condition/stage).

See also Figure S1.

formation (Figures 2J and 2N). By stage 32, the ECs separated in control embryos but remained as aggregates in CASZ1-depleted embryos (Figures 2K and 2O). By stages 36 and 39, the veins of control embryos exhibited well-formed lumens surrounded by *Msr*-positive ECs, whereas the CASZ1-depleted veins remained closed and failed to open even at late stages (Figures 2L, 2M, 2P, and 2Q). Collectively, these studies demonstrate that CASZ1 is required for angiogenic remodeling and lumen morphogenesis during vertebrate vascular development.

Because we previously established that CASZ1 is required for heart development (Christine and Conlon, 2008), we sought to determine whether the vascular requirements for CASZ1 are secondary to its role in cardiac tissue. Taking advantage of the amenability of *Xenopus* embryos to organotypic culture (Mandel et al., 2010), we removed anterior regions of embryos, including all cardiac tissue at a stage prior to heart formation. Culture of explants showed that in the absence of cardiac tissue, the control explants formed vascular networks, as marked by the EC-specific gene *Ami* (Inui and Asashima, 2006), that were indistinguishable from those of unmanipulated embryos, demonstrating that blood flow is not essential for correct patterning of the early vasculature (Figures S1N and S1P). Critically, we observed severe defects in the vascular networks of CASZ1-depleted explants, strongly suggesting that the role of CASZ1 in vascular development is independent of its role in cardiogenesis (Figures S1O and S1Q).

CASZ1 Regulates EC Behavior

To examine vascular development in more detail and determine whether the function of CASZ1 is evolutionarily conserved, we depleted CASZ1 in HUVECs by lentiviral-mediated short hairpin RNA (shRNA, a 16-fold decrease in *Casz1* messenger RNA [mRNA]; Figure 3A). CASZ1-depleted cells displayed a thin and elongated morphology in stark contrast to the characteristic cobblestone appearance of uninfected HUVECs or HUVECs infected with control shRNA (Figure 3B).

To determine the precise requirement for CASZ1 and to characterize the dynamics of CASZ1-depleted HUVECs in real time, we coupled time-lapse imaging with quantitative analysis. Time-lapse movies showed that CASZ1-depleted cells initially adhered to plastic or fibronectin-coated substrates, but a proportion of the cells rounded up and detached (33%; Figure 3C; Movie S1; data not shown). In the CASZ1-depleted HUVECs that adhered, live imaging demonstrated that the elongated morphology resulted from defects in contractility whereby the

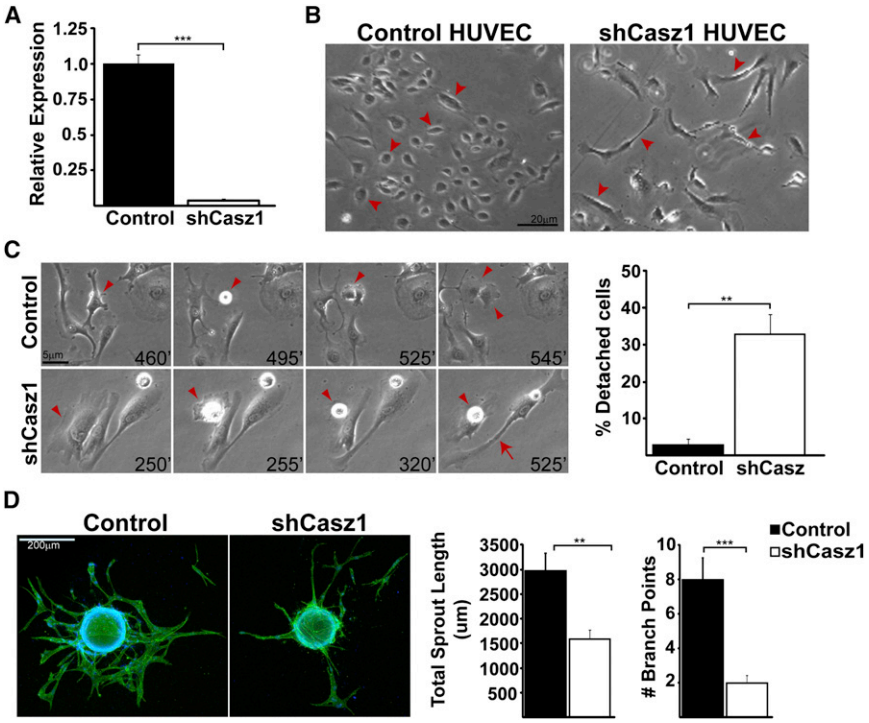

Figure 3. CASZ1 Regulates EC Behavior

(A) mRNA levels of *Casz1* after infection of HUVECs with shCasz1. *Casz1* is decreased by 16-fold. mRNA levels relative to *Rps29* ± SEM. ***$p < 0.001$.

(B) Phase-contrast images of control and shCasz1 HUVECs. Controls display cobblestone-like morphology, whereas CASZ1-depleted cells are thin and elongated (red arrowheads indicate examples of each).

(C) Time-lapse images of control and shCasz1 cells. Red arrowheads indicate dividing control cells and rounded-up CASZ1-depleted cells. Bottom right: Minutes elapsed, taken every 5 min for 24 hr. Red arrow points to an elongated shCasz1 cell with trailing edge defects. Graph represents quantification of cells that round up and detach during imaging. Data represent the mean ± SEM of three experiments conducted on independent batches of shRNA-infected cells (n = 200 cells). **$p < 0.01$.

(D) A sprouting angiogenesis assay was performed with control and CASZ1-depleted HUVECs. On day 6, cultures were fixed and stained for phalloidin (green) and DRAQ5 (blue). Graphs represent the mean ± SEM of total sprout length and number of branch points/bead (n = 11 beads/condition). Experiments were repeated twice on independent batches of shRNA-infected cells. **$p < 0.01$, ***$p < 0.001$.

See also Figure S2 and Movies S1 and S4.

leading edge of CASZ1-depleted cells moved forward without retraction of the trailing edge (Figure 3C; Movie S1). CASZ1-depleted cells also stopped dividing (0% shCasz1 versus 20% control) and we consistently failed to detect any phospho-Histone H3 (pH3)-positive CASZ1-depleted cells (versus 3% control cells; Figure S2A). Using fluorescence-activated cell sorting (FACS), we determined that CASZ1-depleted ECs were blocked at the G1/S transition as seen by the significantly reduced number of cells in S phase (Figure S2B). Blockage in G1/S progression was not associated with programmed cell death as determined by cleaved caspase-3 staining (Figure S2C). Furthermore, the inability of CASZ1-depleted cells to maintain adhesion to the substrate was not a secondary consequence of cell-cycle arrest, as wild-type HUVECs that were chemically treated with mitomycin C did not divide yet remained attached (data not shown). Taken together, these results indicate that CASZ1 has a conserved role in vascular development and is required for EC adhesion, contractility, and G1/S cell-cycle progression.

To assess how adhesive and morphological defects of CASZ1-depleted cells manifest themselves in vessel assembly, we assessed sprouting using a sprouting angiogenesis assay in which HUVEC-coated beads were placed in fibrin. Whereas the control cells displayed elongated sprouts with multiple branch points, similar to our findings in *Xenopus*, the CASZ1-depleted HUVECs had strikingly few sprouts and branches (Figure 3D). Live time-lapse imaging further showed that the CASZ1-depleted cells extended out from beads to initiate sprout formation but then abruptly detached, indicating that CASZ1 is required for proper EC adhesion to promote angiogenic sprouting (Movie S4).

Isolation of the *Egfl7*/miR-126 Locus by CASZ1 Chromatin Immunoprecipitation

To identify direct cardiac and endothelial transcriptional targets of CASZ1, we generated a CASZ1-specific antibody and performed a cloning chromatin immunoprecipitation (ChIP) screen on dissected cardiovascular *Xenopus* tissue (stages 27–29, i.e., the same time and tissue requiring CASZ1; Figure 4A). We identified 110 putative transcriptional targets, including *Egfl7*, an ECM protein that is specifically secreted by ECs and has been shown to be associated with cellular processes similar to those we observed for CASZ1 (i.e., EC adhesion and vessel tubulogenesis; Figure 4B; Table S1; Nichol et al., 2010; Nikolic et al., 2010; Parker et al., 2004).

Recently, studies in mouse and zebrafish identified the evolutionarily conserved miR-126 contained within intron 7 of *Egfl7* (Fish et al., 2008; Kuhnert et al., 2008; Wang et al., 2008). We cloned *Egfl7* and miR-126 from *Xenopus* and showed that EGFL7 is 47% identical to human EGFL7 and 45% identical to mouse EGFL7, whereas *Xenopus* miR-126 is completely (100%) conserved between mouse and human (Fitch et al., 2004; Figure S3A). Genome analysis and characterization of *Xenopus* BACs corresponding to the *Egfl7*/miR-126 locus confirmed that, like other model systems, miR-126 is located within intron 7 of the *Xenopus Egfl7* locus (Figure 4B).

Expression analysis revealed that *Egfl7* is expressed in all major vessels at all stages of vasculogenesis in *Xenopus*, as previously reported for zebrafish, mouse, and human (Figures 4C, 4E, 4G, and 4I; Fitch et al., 2004; Parker et al., 2004). Although *Egfl7* and miR-126 have been reported to be cotranscribed and coexpressed in the vasculature, we found that *Xenopus* miR-126 has an expression pattern distinct from that of *Egfl7*

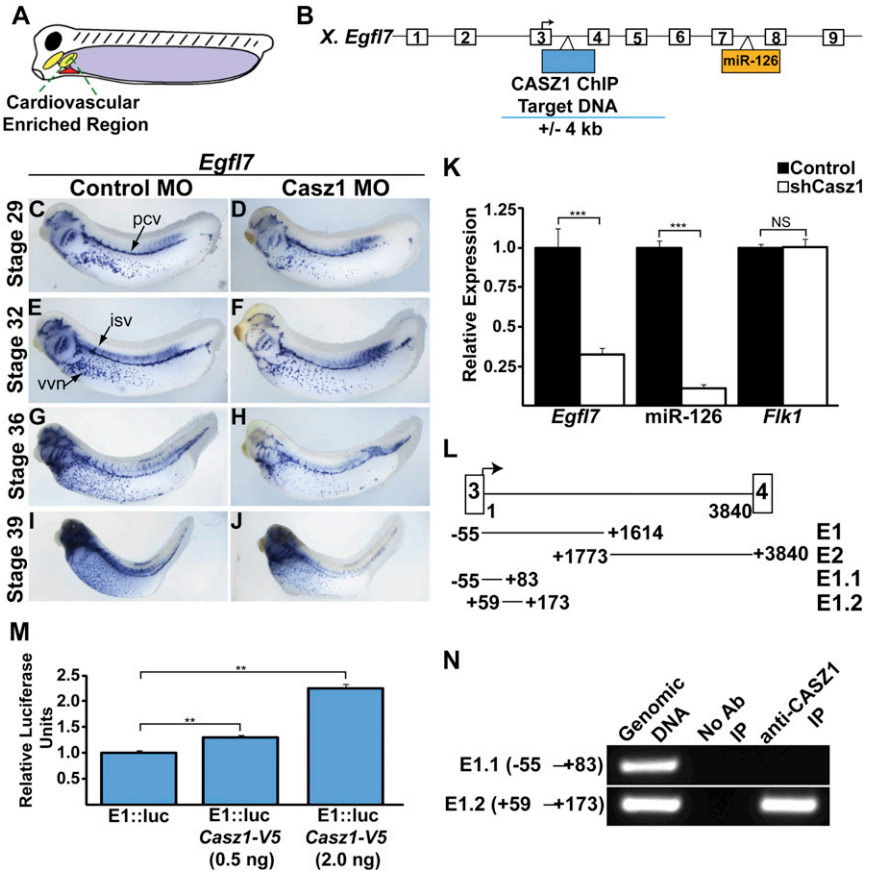

Figure 4. CASZ1 Directly Activates *Egfl7* Transcription

(A) Illustration of cardiovascular-enriched region dissected from *X. tropicalis* for ChIP.

(B) Genomic structure of the *Xenopus Egfl7* locus, denoting a CASZ1 ChIP fragment. White boxes: exons; shaded boxes: miR-126 in intron 7 and intronic region potentially containing CASZ1 element (±4 kb).

(C–J) In situ analysis of *Egfl7* of stage 29–39 control and CASZ1-depleted embryos (lateral view with anterior to the left). Note the downregulation of *Egfl7* in the vvn and isv of CASZ1-depleted embryos.

(K) Relative mRNA expression of *Egfl7*, miR-126, and *Flk1* after infection of HUVECs with shCasz1. mRNA levels relative to *Rps29* ± SEM. ***p < 0.001; NS: not significant.

(L) Schematic demarcating *Egfl7* genomic DNA regions (in bp) tested for transcriptional activation. *E1* (−55 to 1,614) within intron 3 but not *E2* (1,773–3,840) resulted in increased luciferase (luc) activity.

(M) *Egfl7* genomic region *E1* in the presence or absence of *Casz1*. Bars represent fold increase in activity relative to control ± SEM. Experiments were repeated twice on independent batches of embryos; **p < 0.01.

(N) Identification of a 90 bp region endogenously bound by CASZ1 located within a nonoverlapping region of the *E1.2* (113–227) PCR amplicon.

See also Figure S3 and Table S1.

as well as those reported in other species (Fish et al., 2008; Wang et al., 2008). Most notably, miR-126 expression is initiated in ECs at stage 32, slightly later than *Egfl7* (stage 29), and we observed strong expression of miR-126, but not *Egfl7*, in the developing somites (Figures S3B–S3I). Taken together, these data show that the sequence, genomic arrangement, and vascular expression of *Egfl7* and miR-126 are evolutionarily conserved; however, in *Xenopus*, miR-126 has developed additional levels of regulation distinct from *Egfl7*.

Consistent with *Egfl7* being a direct target of CASZ1, analysis in CASZ1-depleted embryos showed that *Egfl7* was initiated but not maintained in vascular tissues at all stages analyzed (Figures 4D, 4F, 4H, and 4J). Consistently, *Egfl7* levels were significantly reduced (by 3-fold) in CASZ1-depleted HUVECs (Figure 4K). We further observed a dramatic reduction in miR-126 (by 9-fold) in CASZ1-depleted HUVECs (Figure 4K). These effects were specific, as the EC marker *Flk1* was unaltered (Figure 4K). However, we did not observe a reduction in miR-126 in CASZ1-depleted *Xenopus* embryos at the mid- and late-tadpole stages (stages 32–39; Figures S3E, S3G, and S3I). Collectively, these studies demonstrate that regulation of *Egfl7* and miR-126 expression in human ECs is dependent on CASZ1, whereas *Xenopus* miR-126 appears to have evolved a CASZ1-independent mechanism of regulation.

Egfl7 Is a Direct Transcriptional Target of CASZ1

To determine whether CASZ1 directly regulates *Egfl7*, we performed in vivo transcriptional assays in which single copies of intronic regions of *Egfl7* corresponding to the putative CASZ1-bound region (introns 2–5) were placed upstream of a basal promoter driving luciferase activity. Of these intronic regions, only the 5′ half of intron 3 (*E1*) resulted in a dose-dependent, reproducible increase in transcriptional activity in response to CASZ1 (Figures 4L and 4M). To determine whether CASZ1 binds endogenously to this element in vivo and to further refine the region within *E1*, we performed ChIP of endogenous CASZ1 from early embryos (stage 32, a time point when CASZ1 is required for *Egfl7* expression). Results showed that CASZ1 binds to nucleotides 59–173 of intron 3 (*E1.2*), but not the most 5′ end of *E1* (*E1.1*; Figure 4N; data not shown). Thus, CASZ1 binds directly to the *Egfl7* locus in vivo and can activate *Egfl7* transcription through a regulatory element within intron 3 of the *Egfl7* locus.

EGFL7 Functions Downstream of CASZ1 to Control Vascular Morphogenesis

To determine whether CASZ1 acts through EGFL7 to regulate EC development, we depleted EGFL7 in embryos using a morpholino that left miR-126 expression intact (Figures S4A–S4E). Strikingly, EGFL7 depletion resulted in vascular phenotypes that phenocopied CASZ1 depletion (Figures 5A–5H and S4F–S4Q). As with CASZ1-depleted embryos, we found a reduction in density of ECs within the vitelline vein network (stage 32; Figures 5A–5D, S4F, S4G, and S4J–S4M). Furthermore, although blood vessels did form in EGFL7-depleted embryos, there was significantly reduced branching and intersomitic vessel

sprouting at later stages (Figures 5E–5H, S4H, S4I, and S4N–S4Q). Quantification of vitelline vein networks at stage 36 revealed results similar to those observed with CASZ1 depletion, i.e., the total length of the vasculature and the number of branch points and intersomitic vessels of EGFL7-depleted embryos was significantly decreased compared with controls (Figure 5I). Furthermore, like the CASZ1-depleted embryos, and in accordance with reports of EGFL7 depletion in zebrafish (Parker et al., 2004), lumens of posterior cardinal veins of EGFL7-depleted embryos failed to form (Figures 5J–5M). Morpholinos targeting the Dicer cleavage site of *Xenopus* pri-miR-126 had no effect on *Egfl7* expression (Figures S5A–S5E) and did not result in gross defects in vessel morphology or patterning, in accordance with reports in zebrafish (Figures S5F–S5U; Fish et al., 2008). Consistently, the lumens of the posterior cardinal veins of miR-126-depleted embryos were indistinguishable from those of controls (Figures S5V–S5Y). Taken together, these results imply that EGFL7 functions downstream of CASZ1 to regulate angiogenesis and vascular remodeling.

Similar to our studies in *Xenopus*, time-lapse imaging of HUVECs revealed that depletion of EGFL7 by shRNA (shEgfl7, 11-fold decrease in mRNA; Figure 5N) phenocopied CASZ1 depletion. Most notably, EGFL7-depleted cells showed adhesion and proliferation defects similar to those observed in CASZ1-depleted cells (Figure 5O; Movie S2), and also displayed an elongated morphology similar to but not as extensive as that observed in CASZ1-depleted cells. The sprouting angiogenesis assay further demonstrated defects similar to those found in CASZ1-depleted cells, i.e., the total length of sprouts and number of branch points were significantly decreased in EGFL7-depleted cells compared with controls (Figure 5P). Live imaging showed that failure to sprout was due to the inability of EGFL7-depleted cells to maintain adhesion (Movie S5). These results were specific, since we observed a minimal effect on expression of *Casz1* or *Flk1* (Figure 5N). Collectively, these studies show that EGFL7 functions downstream of CASZ1 to control vascular morphogenesis in *Xenopus* and humans. In addition, miR-126 does not function downstream of CASZ1 in *Xenopus* vascular development.

EGFL7 and miR-126 Function Downstream of CASZ1 to Regulate Cell Adhesion and Shape

To test whether CASZ1 functions through *Egfl7* or miR-126 to regulate vascular development and morphogenesis in human ECs, we assessed whether restoration of *Egfl7* or miR-126 levels rescues defects associated with CASZ1-depletion. Whereas 29% of cells infected with shCasz1 rounded up and detached, compared with 3% of control cells, infection of CASZ1-depleted cells with adenoviral constructs expressing either human *Egfl7* (Ad-Egfl7) or miR-126 (Ad-miR-126) recovered proper adhesion, as only 7.6% and 1% of cells detached, respectively (Figures 6A, S6A, and S6B; Movie S3). However, restoration of *Egfl7*, but not miR-126, partially rescued EC morphology associated with CASZ1 depletion, as measured by the length-to-width ratio (L:W; Figures 6B and S6C). Restoration of either *Egfl7* or miR-126 failed to rescue proliferation defects (data not shown). Taken together, these studies demonstrate that CASZ1 acts to control EC adhesion through direct transcriptional regulation of *Egfl7* and miR-126. These data further indicate that EGFL7 and miR-126 have distinct functions with regard to cell morphology, since EGFL7, but not miR-126, can rescue cell-shape changes. They also imply that CASZ1 control of G1/S progression occurs by *Egfl7*- and miR-126-independent pathways.

CASZ1 and EGFL7 Regulate RhoA

Previous studies have provided evidence that two of the physiological outputs of the CASZ1/EGFL7 pathway, cell adhesion and morphology, are directly controlled by activation of Rho GTPases. Specifically, RhoA is required for actomyosin-dependent cell contractility and formation of focal adhesions (FAs; Burridge and Wennerberg, 2004; Katoh et al., 2011; Parsons et al., 2010). To identify mechanisms that mediate the physiological function of the CASZ1/EGFL7 pathway, we aimed to determine the relationship between CASZ1/EGFL7 and RhoA. We found that RhoA activity and levels were dramatically diminished in CASZ1- and EGFL7-depleted cells, whereas the levels of other Rho proteins, such as RhoC, were unaltered (Figures 6C, S6D, and S6E). The decrease in RhoA protein occurred at the transcriptional level, as RhoA (but not RhoC) mRNA levels were markedly diminished in both CASZ1- and EGFL7-depleted ECs (Figure 6D). However, RhoB levels were slightly increased, possibly indicating a compensatory mechanism for loss of RhoA (Figure 6D).

We reasoned that a reduction of RhoA expression in CASZ1- and EGFL7-depleted cells would result in concomitantly impaired downstream activity. Consistently, phosphorylation of the regulatory subunit of myosin light chain (p-MLC) was decreased in CASZ1-depleted cells (Figure S6F). To further assess whether decreased RhoA activity directly plays a role in the adhesion and cell-shape defects we observe in CASZ1-depleted cells, we analyzed a panel of cytoskeletal and FA markers. Control cells displayed discrete bundles of F-actin stress fibers, as assayed by phalloidin staining, that contained short or punctate bands of the FA markers vinculin and phosphorylated paxillin (Figure 6E, left panels). However, CASZ1 depletion mimicked treatment with the Rho kinase (ROCK) inhibitor Y-27632, resulting in diffuse actin networks devoid of stress fibers and the failure of vinculin and phosphorylated paxillin to properly localize to adhesion sites on the periphery of the cell (Figure 6E, middle panels; Narumiya et al., 2000). This phenotype was partially rescued by restoration of *Egfl7* levels in CASZ1-depleted cells (Figure 6E, right panels). Taken together, these studies show that CASZ1 acts through the direct transcriptional regulation of EGFL7 to control EC adhesion and shape via the RhoA pathway.

DISCUSSION

In this work we demonstrate an essential and conserved role for the CASZ1/EGFL7/RhoA pathway in vascular patterning. Collectively, these data support a mechanism whereby CASZ1 directly binds to and maintains expression of *Egfl7* in ECs. EGFL7 is then localized extracellularly, where it modulates signals between ECs and the underlying ECM. This in turn is responsible for the transcriptional upregulation and activity of the RhoA GTPase, which ultimately mediates EC contractility and adhesive properties to promote assembly, lumen formation, and functionality of the vasculature (Figure 7).

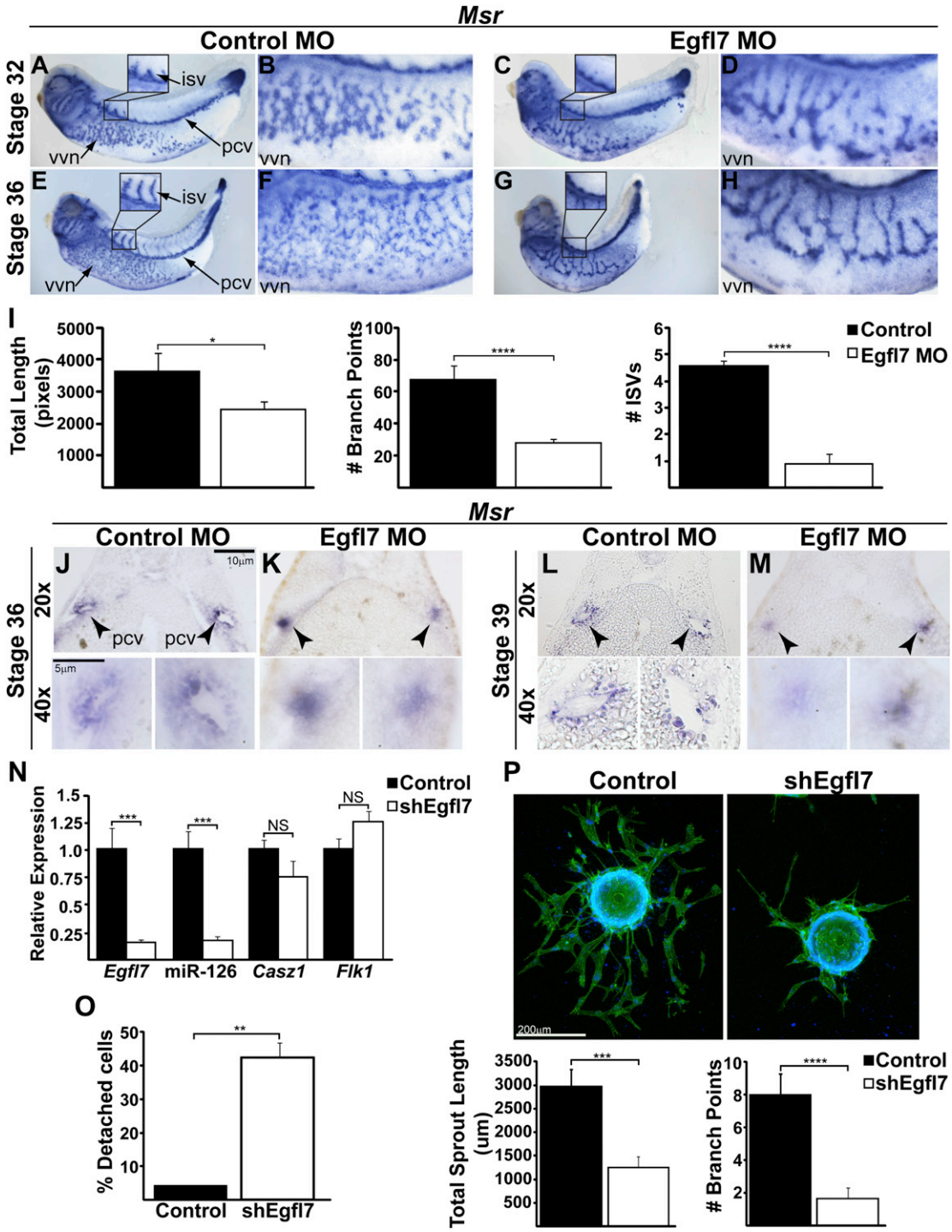

Figure 5. EGFL7 Depletion in Embryos and HUVECs Phenocopies CASZ1 Depletion

(A–H) In situ analysis with EC marker *Msr* of control and EGFL7-depleted embryos (stages 32–36, lateral view with anterior to left). Note the lack of branching in the vvn at stage 32 (A and C: high magnification of the vvn in B and D) and stage 36 (E and G: high magnification of the vvn in F and H); isv sprouting is also impaired (A, C, E, and G). n = 10 embryos/condition/stage, three independent experiments.

(I) Quantification of vascular defects in control and EGFL7-depleted embryos (stage 36) representing total vessel length, number of branch points within the vvn, and number of isv/embryo. Data represent mean ± SEM (n = 7 control and 10 Egfl7 MO embryos). *p < 0.05, **p < 0.01, ****p < 0.0005.

(J–M) Histological analysis reveals lumenless pcv in stage 36 (K) and stage 39 (M) EGFL7-depleted embryos compared to control (J and L). Top: dorsal; bottom: ventral; arrowheads correspond to pcv positions enlarged in lower panels (n = 3 embryos/condition/stage).

(N) mRNA expression of *Egfl7*, miR-126, *Casz1*, *and Flk1* after infection of HUVECs with shEgfl7. *Egfl7* is decreased 11-fold. mRNA levels relative to *Rps29* ± SEM. ***p < 0.001; NS, not significant.

(legend continued on next page)

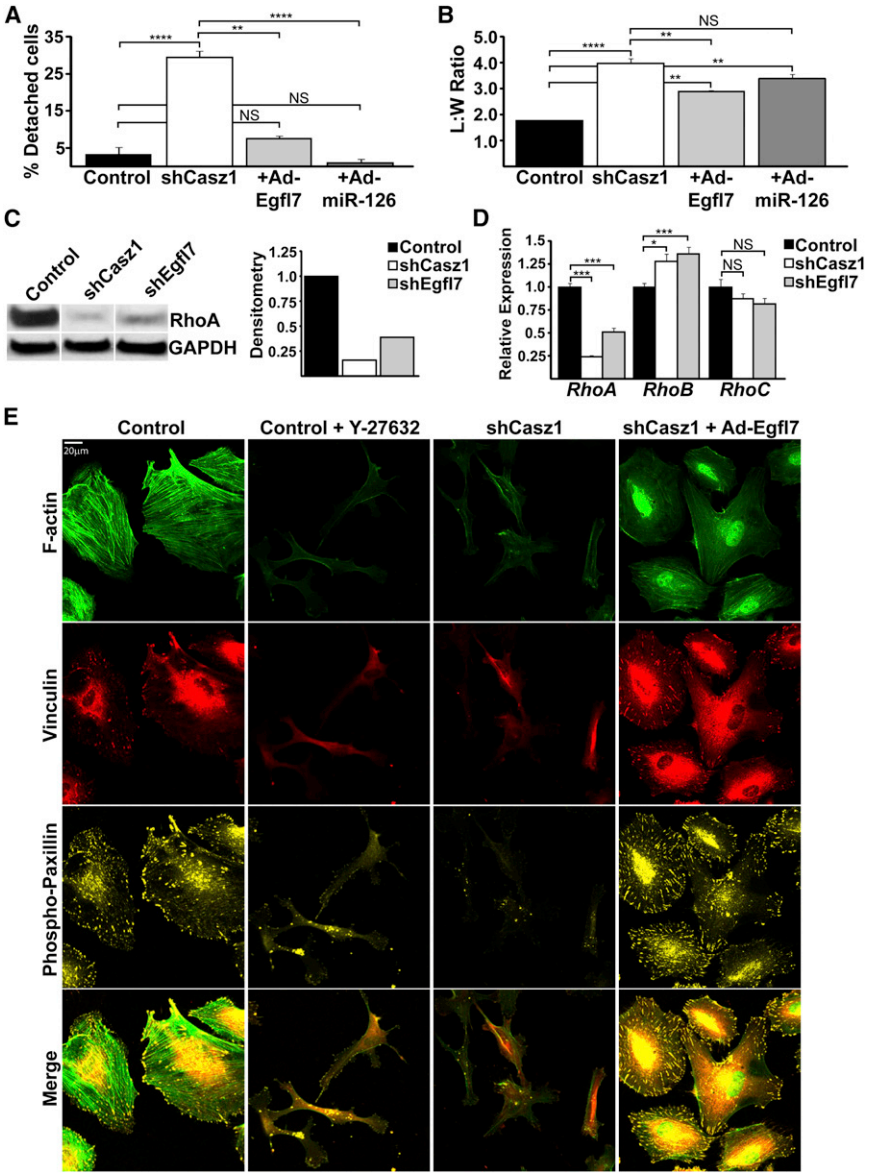

Figure 6. EGFL7 and miR-126 Play Distinct Roles Downstream of CASZ1

(A) Quantification of cells coinfected with shCasz1 and Ad-Egfl7 or Ad-miR-126 that round up and detach versus shCasz1 or control shRNA alone. Data represent the mean ± SEM of two average experiments conducted on independent batches of shRNA-infected cells. n = 100 cells; $^{**}p < 0.01$, $^{****}p < 0.0005$.

(B) Quantification of cell morphology as determined by measuring the L:W ratio. Morphology was improved in cells coinfected with shCasz1 and Ad-Egfl7, but not in cells coinfected with Ad-miR-126. Data represent the mean ± SEM of three experiments conducted on independent batches of shRNA-infected cells. n = 300–600 cells; $^{**}p < 0.01$, $^{****}p < 0.0005$.

(C) RhoA protein expression in shRNA-infected HUVECs. RhoA levels were markedly decreased by depletion of CASZ1 and EGFL7. Graph shows the densitometry of RhoA levels relative to GAPDH.

(D) Relative *RhoA*, *RhoB*, and *RhoC* mRNA expression after shRNA infection. mRNA levels relative to *Rps29* ± SEM. $^{*}p < 0.05$, $^{***}p < 0.001$; NS, not significant.

(E) Stress fibers and FAs disrupted in CASZ1-depleted HUVECs resemble cells treated with ROCK inhibitor Y-27632 (10 μM). Restoration of *Egfl7* in CASZ1-depleted cells rescues proper FA localization. Phalloidin marks F-actin filaments (green), and vinculin (red) and phosphorylated paxillin (yellow) mark FAs.

See also Figure S6 and Movie S3.

CASZ1 Regulates EC Behavior via EGFL7/RhoA to Promote Assembly of a Well-Branched Vascular Network

During embryogenesis, ECs assemble into cord-like structures that undergo further remodeling to form the primary vascular plexus. We have shown that CASZ1 acts through the direct transcriptional regulation of *Egfl7* to promote two critical processes during this period of embryogenesis: sprouting angiogenesis and lumen morphogenesis. The presence of thickened cords lacking lumens in CASZ1-depleted embryos, together with the observation that CASZ1-depleted ECs fail to sprout properly or adhere to extracellular substrates, strongly implies that CASZ1 functions through the EGFL7/RhoA pathway to maintain proper EC adhesion during vessel assembly.

CASZ1 and RhoA

RhoA has been shown to be a central component of pathways that facilitate vascular remodeling. In this regard, RhoA has been demonstrated to be required for stress fiber formation, acting through the actomyosin contractile machinery, and for FA formation (Burridge and Wennerberg, 2004; Chrzanowska-Wodnicka and Burridge, 1996; Katoh et al., 2011; Nobes and Hall, 1995). In accordance with the notion that CASZ1 acts through RhoA to promote proper EC adhesion, we find that depletion of CASZ1 phenocopies inhibition of RhoA and leads to a lack of discrete stress fibers, decreased myosin II activity, and, strikingly, the absence of FA markers at sites of substrate contact. Moreover,

(O) Quantification of cells that round up and detach during imaging. Data represent the mean ± SEM of two experiments conducted on independent batches of shRNA-infected cells. n = 100 cells; $^{**}p < 0.01$.

(P) A sprouting angiogenesis assay was performed with control and EGFL7-depleted HUVECs. On day 6, cultures were fixed and stained for phalloidin (green) and DRAQ5 (blue). Graphs represent the mean ± SEM of total sprout length and number of branch points/bead (n = 11 beads/condition). Experiments were repeated twice on independent batches of shRNA-infected cells. $^{**}p < 0.01$, $^{***}p < 0.001$.

See also Figures S4 and S5 and Movies S2 and S5.

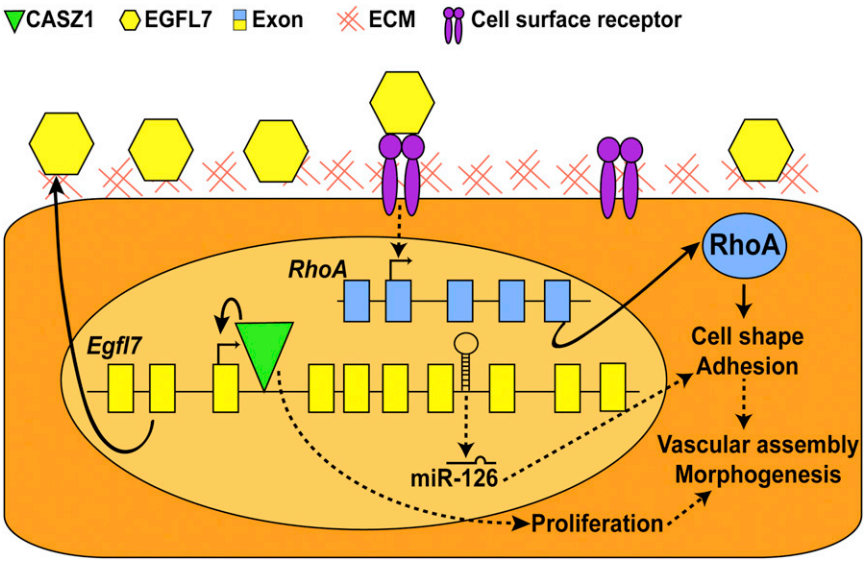

Figure 7. Model Describing CASZ1 Function in ECs

CASZ1 functions by binding to an intronic element within the *Egfl7* locus to activate proper levels of *Egfl7* in endothelial cells. EGFL7 is then secreted to the ECM, where it likely binds cell-surface receptors that signal downstream to activate RhoA expression. Consequently, RhoA signaling modulates endothelial cell behaviors, such as adhesion and contractility, to promote vessel assembly and morphogenesis.

these alterations in EC adherence can all be rescued in a CASZ1-depleted background by restoration of *Egfl7*.

The role of RhoA in tubulogenesis has been controversial. Although some reports have demonstrated that RhoA activity is central for lumen formation, for example in the formation of the mouse dorsal aorta (Strilić et al., 2009), other reports have shown that in culture RhoA is not required for lumen formation, but rather for maintenance of patent vessels (Bayless and Davis, 2002). However, the in vivo relevance of the latter observation has yet to be determined, since the mechanism by which lumens arise in 3D collagen culture differs significantly from that of cord hollowing in vivo (Davis et al., 2007; Strilić et al., 2009). Paradoxically, it was recently demonstrated that RhoA and myosin II activity must be suppressed to promote lumen formation of mouse vessels via negative regulation by Ras interacting protein 1 (RASIP1; Xu et al., 2011). Collectively, these studies along with our present findings imply that a precise level of RhoA activity is required for lumen formation, with either too low or too high activity leading to failure of the vascular cords to hollow and form lumens.

The finding that expression of RhoA protein and mRNA is significantly diminished in CASZ1 and EGFL7-depleted HUVECs indicates that transcriptional control of RhoA is impaired. Very few studies to date have focused on how RhoA transcription is controlled. Although EGFL7 has been shown to interact with lysyl oxidases that are responsible for vascular elastogenesis, as well as some Notch receptors on both ECs and neural stem cells, it is still unclear how these interactions may be influencing RhoA transcription or activity (Lelièvre et al., 2008; Nichol et al., 2010; Schmidt et al., 2009). However, our results would support a mechanism by which CASZ1 modulates RhoA signaling through EGFL7, as restoration of *Egfl7* levels in CASZ1-depleted cells rescues adhesion, proper FA marker localization, and stress fiber formation. It was recently shown that RhoA is directly activated by the Myc-Skp2-Miz1-p300 transcriptional complex (Chan et al., 2010). Given the role of c-Myc in embryonic vascular development and later angiogenic remodeling (Baudino et al., 2002; Kokai et al., 2009; Rodrigues et al., 2008), it will be interesting to investigate whether CASZ1 transcriptional regulation of *Egfl7* plays a direct role in Myc-mediated transcriptional control of RhoA.

Transcriptional Regulation of *Egfl7* and miR-126

Studies on *Egfl7* and miR-126 have identified a 5.4 kb upstream sequence that is sufficient to drive EC-specific expression of a reporter gene in mouse, and mutation of two evolutionarily conserved Ets binding sites within this element eliminated expression in culture (Wang et al., 2008). By showing that CASZ1 is endogenously bound to intron 3 of the *Egfl7* locus in developing embryos and depletion of EGFL7 phenocopies CASZ1 depletion in embryos and HUVECs, we have demonstrated that CASZ1 is required for expression of *Egfl7*. Consistently, we noted that CASZ1 is not required for onset of *Egfl7* expression in embryos but is necessary to maintain that expression. Based on our studies, we favor a model by which Ets factors activate *Egfl7* via an upstream element, and CASZ1 binds to intron 3 and functions to maintain *Egfl7* levels. This model is complementary to findings regarding the role of Ets factors in regulating the spatial pattern of *Egfl7* in mouse (Wang et al., 2008).

Our finding that EGFL7 and miR-126 are both regulated in a CASZ1-dependent manner in humans is congruent with reports in mouse. However, despite the complete conservation of miR-126 across species, we also demonstrate that miR-126 has undergone an evolutionarily divergent and unique means of regulation, as exemplified by our findings that *Xenopus* miR-126 is expressed in domains mutually exclusive to *Egfl7* (i.e., somites) and expression of *Xenopus* miR-126 in the vasculature is CASZ1 independent. These observations are broadly consistent with recent reports that miR-126 transcription can occur independently of host gene transcription through differential intronic promoters (Monteys et al., 2010).

CONCLUSIONS

The vascular system arises via concerted efforts of individual ECs to harness their unique behaviors to assemble into tubular structures. The molecular and cellular mechanisms by which the vasculature arises are still unclear, but we have identified previously unknown roles for CASZ1 in regulating sprouting and morphogenesis. Although the endothelium becomes stabilized and quiescent after embryonic development, vessels remain sensitive to changes in environment due to injury, inflammation, or improper cardiac output, which makes them susceptible to

vascular dysfunction. In this regard, it is interesting that human CASZ1 has been linked to adult vascular diseases such as hypertension (Takeuchi et al., 2010). Events resulting in vascular dysfunction during this disease are associated with aberrant ECM remodeling, proliferation, and adhesion, all of which we have demonstrated to also be dysregulated upon depletion of CASZ1 (Lemarié et al., 2010). Therefore, it will be intriguing to examine the mechanisms by which CASZ1 itself is regulated, and to identify additional transcriptional targets that could trigger the development of innovative therapeutic strategies in cardiovascular disease.

EXPERIMENTAL PROCEDURES

Xenopus Embryo Collection and Morpholino Design

Xenopus embryos were prepared and collected as previously described (Showell et al., 2006). Embryos were staged according to Nieuwkoop and Faber (1967). Morpholino oligonucleotides (MOs) were obtained from Gene Tools. *Casz1*-specific MOs were used as previously described (Christine and Conlon, 2008). *Egfl7*-specific MOs were designed against the acceptor region of *X. laevis* exon 6, and miR-126-specific MOs were designed against the guide dicer region of *X. laevis* (Supplemental Experimental Procedures).

In Situ Hybridization

Whole-mount in situ analysis was carried out as previously described (Harland, 1991) using probes of *Casz1* (Christine and Conlon, 2008), *Msr* (Devic et al., 1996), *Ami* (Inui and Asashima, 2006), *Erg* (cloned from stage 39 *X. laevis* complementary DNA [cDNA]), *Egfl7* (cloned from stage 33–38 *X. tropicalis* cDNA), and *EphrinB2* (cloned from stage 39 *X. laevis* cDNA). miR-126 locked nucleic acid probes were obtained from Exiqon (38523-05) and hybridization was performed according to the manufacturer's instructions at 51°C.

ChIP

Four hundred cardiovascular-enriched regions were dissected from stage 29 *X. tropicalis* embryos and processed for ChIP as previously described (Weinmann and Farnham, 2002; Taranova et al., 2006) with the following exceptions: (1) sonication was carried out with a Branson Digital Sonifier at 20% amplitude (2.5 cycles, 30 s [1 s on/0.5 s off]) to yield 4 kb DNA fragments, (2) affinity-purified rabbit anti-CASZ1 polyclonal antibody (generated in house) was added and incubated overnight at 4°C, and (3) DNA was digested with *NlaIII* (NEB) and ligated into *SphI*-digested (NEB) pUC19 using a DNA ligation kit (Stratagene). Ligated DNA was transformed into NEB10β electrocompetent cells. Transformants were selected by blue/white screening and cultured, and isolated plasmids were sequenced. CASZ1 target DNA sequences were assessed by BLAT analysis using the UCSC *X. tropicalis* Genome Browser (http://genome.ucsc.edu, August 2005 assembly). DNA scaffold location coordinates were imported into the annotated Joint Genome Institute v4.1 database (http://genome.jgi-psf.org/Xentr4/Xentr4.home.html). Validation of targets by ChIP PCR was performed as above with the following exceptions: (1)Thirty stage 32 *X. tropicalis* embryos were collected and processed, and (2) samples were sonicated at 20% amplitude (five cycles, 30 s [1 s on/0.5 s off]) to generate ~300 bp DNA fragments.

In Vivo Transcriptional Assays

Egfl7 intronic regions (introns 2, 3, 4, and 5) were subcloned into pGL3-Promoter firefly luciferase vector (Promega). *X. laevis* embryos were injected at the one-cell stage with 300 pg reporter plasmid and 10 pg Renilla reporter plasmid in the presence or absence of CASZ1 mRNA. Injected embryos were cultured until stage 11.5. Ten injected embryos were lysed in 50 μl Passive Lysis Buffer (Promega) in triplicate. Then 20 μl of cleared lysates was assayed using the Dual-Luciferase Reporter Assay System (Promega).

Cell Culture

Pooled populations of HUVECs (Lonza) were maintained in Complete EBM-2 (Lonza) containing 10% fetal bovine serum (FBS), 100 U/mL penicillin and streptomycin, and used between passages 1 and 6. hCASZ1 was immunoprecipitated from HUVECs using polyclonal rabbit anti-human CASZ1 (LifeSpan Biosciences) and probed by western blot with the same antibody.

shRNA

shRNA viral constructs specific to human *Casz1* and *Egfl7* were obtained from the Open Biosystems TRC1 shRNA library. *Casz1*, *Egfl7*, and control scrambled sequence (Addgene) shRNA lentiviral particles were prepared by the UNC Lentiviral Core Facility. Then 40%–50% confluent HUVECs were infected with 1×10^6 IU lentivirus combined with 10 μg/mL polybrene (Sigma) for 7.5 hr. Infected cells were placed under 1.5 μg/mL puromycin selection for 3 days and processed for further analysis.

Live Time-Lapse Imaging

Cells seeded on uncoated or fibronectin-coated (10 μg/mL) 12-well dishes or embedded in fibrin gel were imaged over 24 hr using an Olympus IX70 inverted microscope encased in Plexiglas housing to control the internal environment (37°C, 5% CO_2, and relative humidity of 60%). Images were collected with the use of Volocity 5.4.1 software.

Immunofluorescence

Cells seeded in chamber slides (BD Falcon) were fixed with cold methanol/acetone, blocked, and incubated with pH3 (Millipore) or cleaved caspase-3 (Cell Signaling) overnight. Cells were incubated with rabbit anti-Cy3 (Sigma), stained with DAPI, and mounted (DakoCytomation). For cytoskeletal staining, cells were serum starved (EBM-2 + 0.75% FBS) overnight and half of the cells were treated with 10 μM Y-27632 (Sigma). The cells were fixed in 4% paraformaldehyde, permeabilized with 0.1% Triton X-100, and incubated overnight with anti-vinculin (Sigma) and anti-phospho-paxillin (pY118; Invitrogen). The cells were incubated with fluorescent secondary antibodies, stained with FITC-conjugated phalloidin (Invitrogen) and DAPI, mounted, and imaged (Zeiss 710 or 700 microscope).

Sprouting Angiogenesis Assay

Sprouting assays were performed as previously described (Nakatsu et al., 2003; Sweet et al., 2012). Cells were stained with phalloidin (FITC) to visualize actin and with DRAQ5 to mark EC nuclei, and imaged (Olympus FLV500 inverted confocal microscope, 20× objective). The assays were used to measure the total length of protruding sprouts and the number of branch points.

Western Blotting

Western blots were performed with 50 μg protein using RhoA (Santa Cruz), p-MLC 2 (Ser 19; Cell Signaling), and RhoC (K-12; Santa Cruz).

Statistical Analysis

Data are expressed as means ± SEM as indicated. Statistical analysis was done by Student's t test and $p < 0.05$ was considered significant.

ACCESSION NUMBERS

The GenBank accession number for *Xenopus laevis* miR-126 reported in this paper is JX393083.

SUPPLEMENTAL INFORMATION

Supplemental Information includes six figures, one table, five movies, and Supplemental Experimental Procedures and can be found with this article online at http://dx.doi.org/10.1016/j.devcel.2013.03.003.

ACKNOWLEDGMENTS

This work is dedicated to the memory of Dr. Larysa H. Pevny, for whose insight, encouragement, and friendship we are extremely grateful. We thank the faculty of the Microscopy Services Laboratory at the University of North Carolina for microscopy help and John Wallingford, Mark Peifer, and Keith Burridge for helpful discussions and critical readings of manuscript. This work was supported by grants to F.L.C. from the NIH/NHLBI (RO1 DE018825 and RO1 HL089641). N.M.A. and K.S.C. were supported by AHA awards.

Received: July 16, 2012
Revised: January 22, 2013
Accepted: March 1, 2013
Published: April 29, 2013

REFERENCES

Baltzinger, M., Mager-Heckel, A.M., and Remy, P. (1999). Xl erg: expression pattern and overexpression during development plead for a role in endothelial cell differentiation. Dev. Dyn. *216*, 420–433.

Barton, K., Muthusamy, N., Fischer, C., Ting, C.N., Walunas, T.L., Lanier, L.L., and Leiden, J.M. (1998). The Ets-1 transcription factor is required for the development of natural killer cells in mice. Immunity *9*, 555–563.

Baudino, T.A., McKay, C., Pendeville-Samain, H., Nilsson, J.A., Maclean, K.H., White, E.L., Davis, A.C., Ihle, J.N., and Cleveland, J.L. (2002). c-Myc is essential for vasculogenesis and angiogenesis during development and tumor progression. Genes Dev. *16*, 2530–2543.

Bayless, K.J., and Davis, G.E. (2002). The Cdc42 and Rac1 GTPases are required for capillary lumen formation in three-dimensional extracellular matrices. J. Cell Sci. *115*, 1123–1136.

Burridge, K., and Wennerberg, K. (2004). Rho and Rac take center stage. Cell *116*, 167–179.

Campagnolo, L., Leahy, A., Chitnis, S., Koschnick, S., Fitch, M.J., Fallon, J.T., Loskutoff, D., Taubman, M.B., and Stuhlmann, H. (2005). EGFL7 is a chemoattractant for endothelial cells and is up-regulated in angiogenesis and arterial injury. Am. J. Pathol. *167*, 275–284.

Carmeliet, P. (2003). Angiogenesis in health and disease. Nat. Med. *9*, 653–660.

Carmeliet, P., and Jain, R.K. (2011). Molecular mechanisms and clinical applications of angiogenesis. Nature *473*, 298–307.

Chan, C.H., Lee, S.W., Li, C.F., Wang, J., Yang, W.L., Wu, C.Y., Wu, J., Nakayama, K.I., Kang, H.Y., Huang, H.Y., et al. (2010). Deciphering the transcriptional complex critical for RhoA gene expression and cancer metastasis. Nat. Cell Biol. *12*, 457–467.

Christine, K.S., and Conlon, F.L. (2008). Vertebrate CASTOR is required for differentiation of cardiac precursor cells at the ventral midline. Dev. Cell *14*, 616–623.

Chrzanowska-Wodnicka, M., and Burridge, K. (1996). Rho-stimulated contractility drives the formation of stress fibers and focal adhesions. J. Cell Biol. *133*, 1403–1415.

Cleaver, O., Tonissen, K.F., Saha, M.S., and Krieg, P.A. (1997). Neovascularization of the Xenopus embryo. Dev. Dyn. *210*, 66–77.

Cox, C.M., D'Agostino, S.L., Miller, M.K., Heimark, R.L., and Krieg, P.A. (2006). Apelin, the ligand for the endothelial G-protein-coupled receptor, APJ, is a potent angiogenic factor required for normal vascular development of the frog embryo. Dev. Biol. *296*, 177–189.

Davis, G.E., Koh, W., and Stratman, A.N. (2007). Mechanisms controlling human endothelial lumen formation and tube assembly in three-dimensional extracellular matrices. Birth Defects Res. C Embryo Today *81*, 270–285.

De Val, S. (2011). Key transcriptional regulators of early vascular development. Arterioscler. Thromb. Vasc. Biol. *31*, 1469–1475.

De Val, S., and Black, B.L. (2009). Transcriptional control of endothelial cell development. Dev. Cell *16*, 180–195.

Devic, E., Paquereau, L., Vernier, P., Knibiehler, B., and Audigier, Y. (1996). Expression of a new G protein-coupled receptor X-msr is associated with an endothelial lineage in *Xenopus laevis*. Mech. Dev. *59*, 129–140.

Fish, J.E., Santoro, M.M., Morton, S.U., Yu, S., Yeh, R.F., Wythe, J.D., Ivey, K.N., Bruneau, B.G., Stainier, D.Y., and Srivastava, D. (2008). miR-126 regulates angiogenic signaling and vascular integrity. Dev. Cell *15*, 272–284.

Fitch, M.J., Campagnolo, L., Kuhnert, F., and Stuhlmann, H. (2004). Egfl7, a novel epidermal growth factor-domain gene expressed in endothelial cells. Dev. Dyn. *230*, 316–324.

Harland, R.M. (1991). In situ hybridization: an improved whole mount method for Xenopus embryos. Methods Cell Biol. *36*, 685–695.

Inui, M., and Asashima, M. (2006). A novel gene, Ami is expressed in vascular tissue in Xenopus laevis. Gene Expr. Patterns *6*, 613–619.

Katoh, K., Kano, Y., and Noda, Y. (2011). Rho-associated kinase-dependent contraction of stress fibres and the organization of focal adhesions. J. R. Soc. Interface *8*, 305–311.

Kokai, E., Voss, F., Fleischer, F., Kempe, S., Marinkovic, D., Wolburg, H., Leithäuser, F., Schmidt, V., Deutsch, U., and Wirth, T. (2009). Myc regulates embryonic vascular permeability and remodeling. Circ. Res. *104*, 1151–1159.

Kuhnert, F., Mancuso, M.R., Hampton, J., Stankunas, K., Asano, T., Chen, C.Z., and Kuo, C.J. (2008). Attribution of vascular phenotypes of the murine Egfl7 locus to the microRNA miR-126. Development *135*, 3989–3993.

Lelièvre, E., Lionneton, F., Soncin, F., and Vandenbunder, B. (2001). The Ets family contains transcriptional activators and repressors involved in angiogenesis. Int. J. Biochem. Cell Biol. *33*, 391–407.

Lelièvre, E., Hinek, A., Lupu, F., Buquet, C., Soncin, F., and Mattot, V. (2008). VE-statin/egfl7 regulates vascular elastogenesis by interacting with lysyl oxidases. EMBO J. *27*, 1658–1670.

Lemarié, C.A., Tharaux, P.L., and Lehoux, S. (2010). Extracellular matrix alterations in hypertensive vascular remodeling. J. Mol. Cell. Cardiol. *48*, 433–439.

Levine, A.J., Munoz-Sanjuan, I., Bell, E., North, A.J., and Brivanlou, A.H. (2003). Fluorescent labeling of endothelial cells allows in vivo, continuous characterization of the vascular development of Xenopus laevis. Dev. Biol. *254*, 50–67.

Levy, D., Ehret, G.B., Rice, K., Verwoert, G.C., Launer, L.J., Dehghan, A., Glazer, N.L., Morrison, A.C., Johnson, A.D., Aspelund, T., et al. (2009). Genome-wide association study of blood pressure and hypertension. Nat. Genet. *41*, 677–687.

Mandel, E.M., Kaltenbrun, E., Callis, T.E., Zeng, X.X., Marques, S.R., Yelon, D., Wang, D.Z., and Conlon, F.L. (2010). The BMP pathway acts to directly regulate Tbx20 in the developing heart. Development *137*, 1919–1929.

Monteys, A.M., Spengler, R.M., Wan, J., Tecedor, L., Lennox, K.A., Xing, Y., and Davidson, B.L. (2010). Structure and activity of putative intronic miRNA promoters. RNA *16*, 495–505.

Nakatsu, M.N., Sainson, R.C., Aoto, J.N., Taylor, K.L., Aitkenhead, M., Pérez-del-Pulgar, S., Carpenter, P.M., and Hughes, C.C. (2003). Angiogenic sprouting and capillary lumen formation modeled by human umbilical vein endothelial cells (HUVEC) in fibrin gels: the role of fibroblasts and Angiopoietin-1. Microvasc. Res. *66*, 102–112.

Narumiya, S., Ishizaki, T., and Uehata, M. (2000). Use and properties of ROCK-specific inhibitor Y-27632. Methods Enzymol. *325*, 273–284.

Nichol, D., Shawber, C., Fitch, M.J., Bambino, K., Sharma, A., Kitajewski, J., and Stuhlmann, H. (2010). Impaired angiogenesis and altered Notch signaling in mice overexpressing endothelial Egfl7. Blood *116*, 6133–6143.

Nieuwkoop, P.D., and Faber, J. (1967). Normal Table of *Xenopus laevis* (Daudin) (Amsterdam: North Holland).

Nikolic, I., Plate, K.H., and Schmidt, M.H. (2010). EGFL7 meets miRNA-126: an angiogenesis alliance. J. Angiogenes Res. *2*, 9.

Nobes, C.D., and Hall, A. (1995). Rho, rac, and cdc42 GTPases regulate the assembly of multimolecular focal complexes associated with actin stress fibers, lamellipodia, and filopodia. Cell *81*, 53–62.

Parker, L.H., Schmidt, M., Jin, S.W., Gray, A.M., Beis, D., Pham, T., Frantz, G., Palmieri, S., Hillan, K., Stainier, D.Y., et al. (2004). The endothelial-cell-derived secreted factor Egfl7 regulates vascular tube formation. Nature *428*, 754–758.

Parsons, J.T., Horwitz, A.R., and Schwartz, M.A. (2010). Cell adhesion: integrating cytoskeletal dynamics and cellular tension. Nat. Rev. Mol. Cell Biol. *11*, 633–643.

Patan, S. (2000). Vasculogenesis and angiogenesis as mechanisms of vascular network formation, growth and remodeling. J. Neurooncol. *50*, 1–15.

Potente, M., Gerhardt, H., and Carmeliet, P. (2011). Basic and therapeutic aspects of angiogenesis. Cell *146*, 873–887.

Rodrigues, C.O., Nerlick, S.T., White, E.L., Cleveland, J.L., and King, M.L. (2008). A Myc-Slug (Snail2)/Twist regulatory circuit directs vascular development. Development *135*, 1903–1911.

Schmidt, M.H., Bicker, F., Nikolic, I., Meister, J., Babuke, T., Picuric, S., Müller-Esterl, W., Plate, K.H., and Dikic, I. (2009). Epidermal growth factor-like domain 7 (EGFL7) modulates Notch signalling and affects neural stem cell renewal. Nat. Cell Biol. *11*, 873–880.

Showell, C., Christine, K.S., Mandel, E.M., and Conlon, F.L. (2006). Developmental expression patterns of Tbx1, Tbx2, Tbx5, and Tbx20 in Xenopus tropicalis. Dev. Dyn. *235*, 1623–1630.

Strilić, B., Kucera, T., Eglinger, J., Hughes, M.R., McNagny, K.M., Tsukita, S., Dejana, E., Ferrara, N., and Lammert, E. (2009). The molecular basis of vascular lumen formation in the developing mouse aorta. Dev. Cell *17*, 505–515.

Sweet, D.T., Chen, Z., Wiley, D.M., Bautch, V.L., and Tzima, E. (2012). The adaptor protein Shc integrates growth factor and ECM signaling during postnatal angiogenesis. Blood *119*, 1946–1955.

Takeuchi, F., Isono, M., Katsuya, T., Yamamoto, K., Yokota, M., Sugiyama, T., Nabika, T., Fujioka, A., Ohnaka, K., Asano, H., et al. (2010). Blood pressure and hypertension are associated with 7 loci in the Japanese population. Circulation *121*, 2302–2309.

Taranova, O.V., Magness, S.T., Fagan, B.M., Wu, Y., Surzenko, N., Hutton, S.R., and Pevny, L.H. (2006). SOX2 is a dose-dependent regulator of retinal neural progenitor competence. Genes Dev. *20*, 1187–1202.

Wang, S., Aurora, A.B., Johnson, B.A., Qi, X., McAnally, J., Hill, J.A., Richardson, J.A., Bassel-Duby, R., and Olson, E.N. (2008). The endothelial-specific microRNA miR-126 governs vascular integrity and angiogenesis. Dev. Cell *15*, 261–271.

Warkman, A.S., Zheng, L., Qadir, M.A., and Atkinson, B.G. (2005). Organization and developmental expression of an amphibian vascular smooth muscle alpha-actin gene. Dev. Dyn. *233*, 1546–1553.

Weinmann, A.S., and Farnham, P.J. (2002). Identification of unknown target genes of human transcription factors using chromatin immunoprecipitation. Methods *26*, 37–47.

Xu, K., Sacharidou, A., Fu, S., Chong, D.C., Skaug, B., Chen, Z.J., Davis, G.E., and Cleaver, O. (2011). Blood vessel tubulogenesis requires Rasip1 regulation of GTPase signaling. Dev. Cell *20*, 526–539.